AIP | Journal of Applied Physics

Low spin-wave damping in amorphous Co40Fe40B20 thin films

A. Conca, J. Greser, T. Sebastian, S. Klingler, B. Obry et al.

Citation: J. Appl. Phys. **113**, 213909 (2013); doi: 10.1063/1.4808462
View online: http://dx.doi.org/10.1063/1.4808462
View Table of Contents: http://jap.aip.org/resource/1/JAPIAU/v113/i21
Published by the American Institute of Physics.

JOURNAL OF APPLIED PHYSICS **113**, 213909 (2013)

Low spin-wave damping in amorphous $Co_{40}Fe_{40}B_{20}$ thin films

A. Conca,[a] J. Greser, T. Sebastian, S. Klingler, B. Obry, B. Leven, and B. Hillebrands
Fachbereich Physik and Forschungszentrum OPTIMAS, Technische Universität Kaiserslautern, 67663 Kaiserslautern, Germany

(Received 28 March 2013; accepted 17 May 2013; published online 7 June 2013)

A characterization of the magnetic properties of amorphous $Co_{40}Fe_{40}B_{20}$ thin films, developed for low damping applications in magnon spintronics, using vector network analyzer ferromagnetic resonance (VNA-FMR) and the magneto-optical Kerr effect is presented. Our films show a very weak uniaxial anisotropy and a low Gilbert damping parameter ($\alpha = 0.0042$). The saturation magnetization M_S extracted from the FMR measurements is 1250 kA/m. The frequency dependence of the first perpendicular standing spin waves mode on the applied magnetic field is used to determine the exchange constant A for this alloy resulting in a value of 1.5×10^{-11} J/m. These values are discussed in comparison to literature values for different CoFeB compositions and other related alloys. © *2013 AIP Publishing LLC*. [http://dx.doi.org/10.1063/1.4808462]

I. INTRODUCTION

The magnetic community has in the last years been witness of a large activity in the search and characterization of low-damping ferromagnetic thin films. Such materials are required for spin-wave propagation and manipulation investigations where the reduced spin-wave dissipation leads to a larger decay length. Additionally, low-damping thin films are also of importance for spin-transfer switching devices, including spin-torque nano-oscillators (STNO) and for other applications in the field of magnon spintronics. Currently, yttrium iron garnet (YIG) and NiFe films are used for these purposes due to the low damping values. However, both materials show critical disadvantages. The production of YIG films is complicated and cost intensive and incompatible with current CMOS technology. Additionally, the fabrication of microstructures in YIG films is extremely difficult. For NiFe, the decay lengths are in the order of micrometers which difficult any information transfer and process based on spin-waves or spin currents. Heusler compounds have attracted a large interest in this area and low damping values have been reported together with increased decay lengths and the pronounced occurrence of nonlinear effects.[1,2] However, an annealing step at high temperature and a single crystalline substrate are typical requirements for high quality films. Therefore, we propose an alternative with CoFeB with simplified fabrication process. CoFeB is commonly used in the fabrication of magnetic tunneling junctions, providing high TMR ratios in combination with MgO barriers.[3,4]

II. FILM DEPOSITION AND QUASI-STATIC CHARACTERIZATION

Here, we report on a characterization of $Co_{40}Fe_{40}B_{20}$ (CoFeB hereafter) thin films deposited by magnetron rf sputtering on SiO_2 substrates in a chamber with a base pressure of 5×10^{-7} millbars. The Ar pressure during deposition was 4.7×10^{-3} millibars with a gas flow of 10 sccm. The quasi-static anisotropic switching properties were measured with a magneto-optical Kerr (MOKE) effect setup in longitudinal geometry with a spatial resolution of about 100 μm and a laser wavelength of 635 nm. A rotational stage allows for magnetization reversal measurements for any in-plane orientation of the sample with respect to the applied field. The dynamic properties and material parameters were studied by measuring the ferromagnetic resonance using a stripline-vector network analyzer (VNA-FMR). In this work, all films were studied as-deposited, i.e., without an annealing step. The surface was studied with *ex-situ* AFM proving a very smooth topology with a root mean square roughness parameter $S_q = 0.4$ nm for a film with a thickness of 75 nm.

The CoFeB thin films are magnetically soft with a well defined but weak uniaxial anisotropy, as shown in Fig. 1(a), where the measured angular dependence of the coercive field H_C for a 75 nm film is plotted. The value of H_C along the easy axis lies below 0.3 mT. Since CoFeB is expected to be amorphous in the as-deposited state, the orientation of the easy axis is defined by the rest magnetic field created by the sputtering sources in the deposition chamber. Sample hysteresis curves along the easy (0°) and hard (90°) axes are shown in Fig. 1(b). Additionally, the curve for the orientation with maximal H_C is also drawn.

III. SATURATION MAGNETIZATION AND GILBERT DAMPING PARAMETER

Figure 2(a) shows the dependence of the FMR frequency on the external field for a 75 nm thick film. A sample spectrum is plotted on graph (b), showing directly the normalized S_{12} and S_{11} parameters, proportional to the absorbed and reflected microwave power. In order to separate the magnetic signal of the sample from the electrical signal of the whole system including also the stripline, cables, and electrical contacts, a reference spectrum is taken and used for normalization. For this purpose, the magnetic field is set to a value large enough to shift the FMR frequency well above the frequency range used in the following measurements.

The data shown in Fig. 2(a) have been fitted (red line) using Kittel's formula[8]

[a]Electronic mail: conca@physik.uni-kl.de

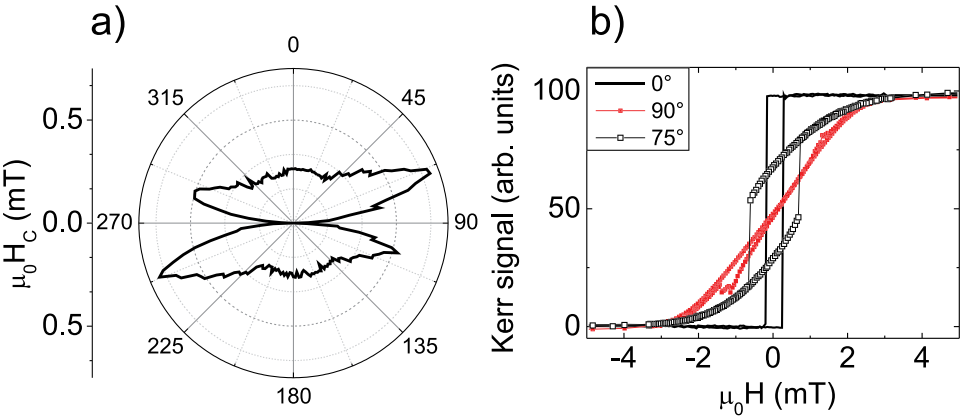

FIG. 1. (a) Angular dependence of the in-plane coercive field H_C of a 75 nm $Co_{40}Fe_{40}B_{20}$ thin film deposited on a SiO_x substrate. (b) Sample hysteresis loops along the easy (0°) and hard (90°) axes. The hysteresis loop for the orientation with maximal H_C (75°) is also plotted.

$$f_{\mathrm{FMR}} = \frac{|\gamma|\mu_0}{2\pi}\sqrt{(H_{\mathrm{ext}} + H_{\mathrm{ani}})(H_{\mathrm{ext}} + H_{\mathrm{ani}} + M_{\mathrm{S}})}, \quad (1)$$

where H_{ext}, H_{ani} are the applied and anisotropy magnetic field, respectively, M_{S} is the saturation magnetization, and γ is the gyromagnetic ratio of the free electron. Taking into account the varying values from sample to sample, we determine M_{S} for $Co_{40}Fe_{40}B_{20}$ to be 1250 ± 30 kA/m. Literature values for the same stoichiometry were found to be 1000 kA/m (Ref. 6) or 1230 kA/m (Ref. 7) for as-deposited films. A clear reason for this large discrepancy was not found.

Further information about the dynamic properties of the CoFeB films is extracted from the FMR data. The width ΔH of the FMR peak in the field-space is related to the dimensionless Gilbert damping parameter α[9]

$$\Delta H = \Delta H_0 + \frac{4\pi\alpha f}{\gamma}. \quad (2)$$

An example of a FMR spectrum is plotted in Fig. 3(b). The procedure described by Kalarickal *et al.*[9] is used to calculate these spectra from the measured data shown in Fig. 2. Fig. 3(a) shows the dependence of ΔH on the FMR frequency which nicely follows the linear behavior described in Eq. (2). The red line represents the result of a linear fit to the data. A very low value of $\alpha = 0.0042$ for the Gilbert damping parameter is obtained for our amorphous CoFeB films. This value is smaller than the measured one for permalloy films (0.007),[10] and it is comparable to the low values obtained for epitaxial films of some Co-based full-Heusler alloys like Co_2MnAl (0.006), Co_2MnSi (0.006), or $Co_2Fe_{0.4}Mn_{0.6}Si$ (0.003).[10–13] The low value for amorphous $Co_{40}Fe_{40}B_{20}$ and the fact that the film growth is possible on amorphous SiO_x wafers make this material suitable for fields where a low damping is of advantage, such as in spin-wave propagation experiments. A similar value for α has been also measured for this same alloy,[18] however, for films annealed for 4 h at 310 °C (see Table I). For as-deposited films, a different study provides a value of 0.013,[19] which is three times larger than the obtained result in this work. Since both values for α were obtained by different groups, no conclusion about the influence of the annealing temperature on this parameter can be extracted. Our result shows that it is possible to obtain a very low damping parameter even without an annealing step.

IV. EXCHANGE CONSTANT

The same VNA-FMR configuration used for the determination of the Gilbert damping parameter is also applied to the determination of the exchange constant A. For this purpose, the field dependence of the frequency of the first standing perpendicular spin wave mode (PSSW) is measured. Films with thicknesses between 150 and 200 nm are used. The reason for the choice of thicker films for the estimation of A in comparison to the determination of the damping parameter lies in the limited sensitivity of the experiment which does not allow for the detection of any PSSW mode in 75 nm thick films.

Figure 4(a) shows an absorption spectrum of a 158 nm thick CoFeB film where the peaks corresponding to the ferromagnetic resonance and to the first PSSW mode are identified. The dependence of the frequency of both peaks on the applied magnetic field is plotted in Fig. 4(b). The

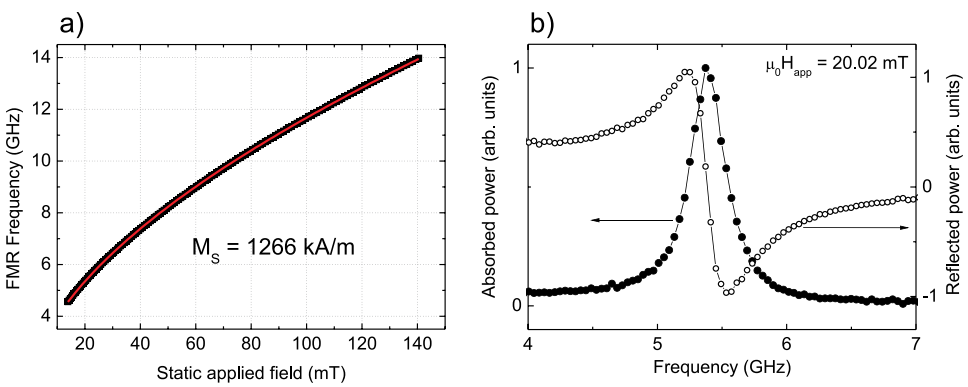

FIG. 2. (a) Dependence of the FMR frequency on the external applied magnetic field for a 75 nm $Co_{40}Fe_{40}B_{20}$ thin film deposited on a SiO_x substrate. The red line represents a fit to the Kittel's formula. (b) Single example FMR spectrum showing directly the normalized S_{12} and S_{11} parameters, proportional to the absorbed and reflected microwave power.

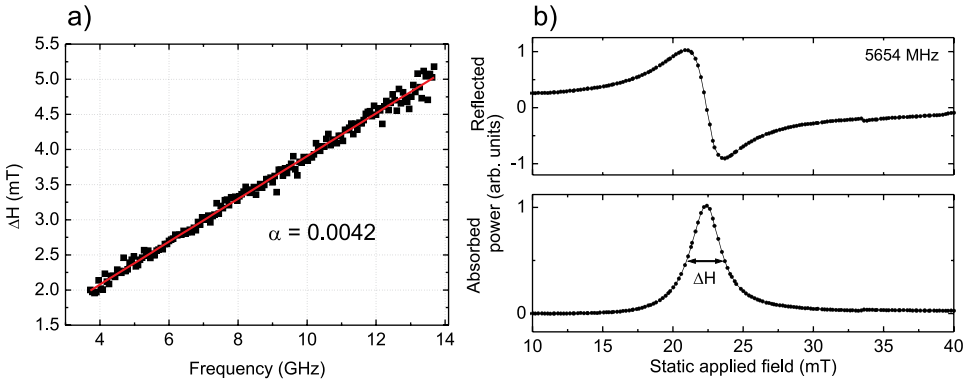

FIG. 3. (a) Dependence of the width ΔH of the ferromagnetic resonance on the FMR frequency for a 75 nm thick $Co_{40}Fe_{40}B_{20}$ film. The red line represents a linear fit to the data from which the Gilbert damping parameter α is extracted. (b) Single example FMR spectrum in the field space calculated following Kalarickal.[9]

frequency of the PSSW modes can be calculated following the expression:[11]

$$f_{\mathrm{pssw}} = \frac{|\gamma|\mu_0}{2\pi}\left[\left(H_{\mathrm{ext}} + \frac{2A}{M_S}\left(\frac{p\pi}{d}\right)^2\right) \times \left(H_{\mathrm{ext}} + \frac{2A}{M_S}\left(\frac{p\pi}{d}\right)^2 + 4\pi M_S\right)\right]^{1/2}, \quad (3)$$

where p is the order of the PSSW mode, A is the exchange constant, and d is the thickness of the film. This expression with $p = 1$ is fitted to the data for the first PSSW mode (red line in Fig. 4(b)) and a value for A is extracted. Taking again into account the dispersion for the results obtained from several samples and the uncertainty in the film thickness (± 6 nm), a value of $A = (1.5 \pm 0.4) \times 10^{-11}$ J/m is obtained. An additional measurement performed using a Brillouin light scattering (BLS) setup described elsewhere in Refs. 16 and 17 on a 75 nm thick CoFeB film provides a confirmation of this value. A value of $A = (1.3 \pm 0.2) \times 10^{-11}$ J/m is determined.

The measured value for A is surprisingly low compared to related alloys. Table I shows literature values for Co, CoFe, and CoFeB with different compositions. The values for the three known crystalline structures for Co are well above 2×10^{-11} J/m. This is also true for the values for the CoFe alloys. For some compositions, the measured value for A is even above 3×10^{-11} J/m reaching 3.84×10^{-11} J/m for $Co_{47}Fe_{53}$. It must be pointed out that the values from Refs. 5 and 15 may not be comparable since the growth conditions are very different (ion beam deposition from a single target and molecular beam epitaxy from different sources). The reason for the low value for A is unclear though it may be related to the higher B content in the alloy. Additionally, the deposition technique used in this work (sputtering) is different from the used one for the result for $Co_{72}Fe_{18}B_{10}$ in Table I (ion beam deposition). In any case, this value has to be taken into account in the design of devices such as sensors, MRAM or spin-torque-transfer (STT) devices based on this alloy and in micromagnetic simulations studying their behavior and performance.

TABLE I. Comparison of the literature values of the exchange constant A for CoFeB and related alloys and the Gilbert damping parameter α for different CoFeB compositions with the values obtained in this work.

	A (10^{-11} J/m)	α (10^{-3})	
Co (hcp)	2.85		Ref. 14
Co (fcc)	2.73		Ref. 14
Co (bcc)	2.12		Ref. 14
$Co_{80}Fe_{20}$ as dep.	2.61		Ref. 5
$Co_{80}Fe_{20}$ anneal.	2.75		Ref. 5
$Co_{37}Fe_{63}$ epitaxial	3.21		Ref. 15
$Co_{47}Fe_{53}$ epitaxial	3.84		Ref. 15
$Co_{72}Fe_{18}B_{10}$ as dep.	2.84	6	Ref. 5
$Co_{72}Fe_{18}B_{10}$ anneal.	…	32	Ref. 5
$Co_{40}Fe_{40}B_{20}$ anneal.	…	4.0	Ref. 18
$Co_{40}Fe_{40}B_{20}$ as dep.	…	13	Ref. 19
$Co_{40}Fe_{40}B_{20}$ as dep.	1.5	4.2	This paper

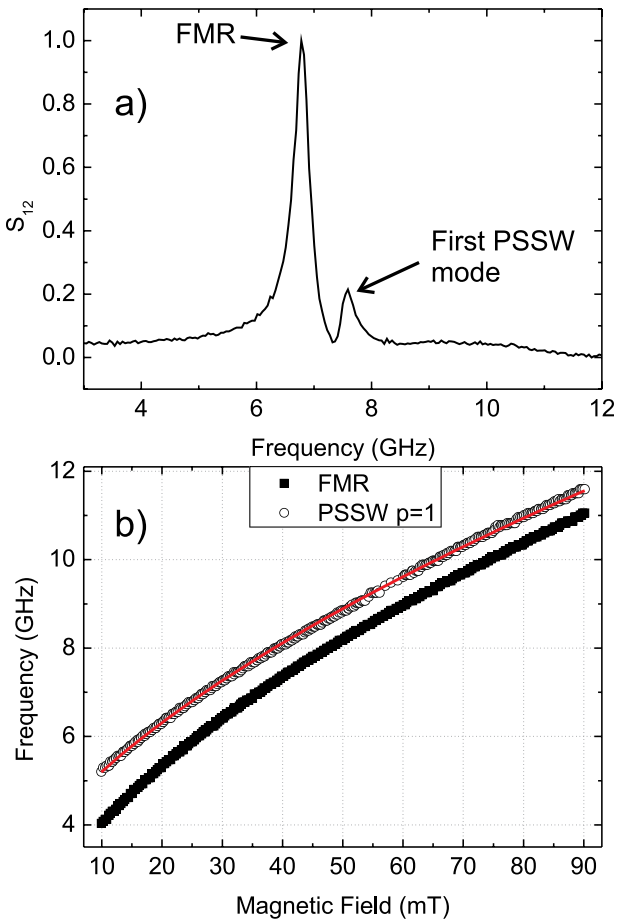

FIG. 4. (a) Single example FMR spectrum showing directly the normalized S_{12} parameter proportional to the absorbed microwave power for a 158 nm thick $Co_{40}Fe_{40}B_{20}$ film. The peaks corresponding to the FMR and to the first PSSW mode are identified. (b) Dependence of the FMR and the first PSSW mode frequency on the applied magnetic field. The red line represents a fit using Eq. (3).

V. SUMMARY

Due to the low measured Gilbert damping parameter ($\alpha = 0.0042$), $Co_{40}Fe_{40}B_{20}$ is a very good candidate for spin-wave propagation and manipulation investigations and for spin-transfer switching studies. The fact that no annealing step is required to achieve a low damping and that the growth is possible on SiO_x substrates are additional advantages which strongly simplify the deposition of samples. The exchange constant A is measured resulting in a value lower than in related alloys.

ACKNOWLEDGMENTS

Financial support by the state of Rhineland-Palatinate (MBWWK and MWKEL) and by the European Regional Development Fund (ERDF) in the frame of the Spintronic Technology Platform (STeP) is acknowledged. The authors wish to thank the Nano Structuring Center (NSC) in Kaiserslautern and T. Brächer for their support in thin film preparation.

[1]T. Sebastian, Y. Ohdaira, T. Kubota, P. Pirro, T. Brächer, K. Vogt, A. A. Serga, H. Naganuma, M. Oogane, Y. Ando, and B. Hillebrands, Appl. Phys. Lett. **100**, 112402 (2012).
[2]T. Sebastian, T. Brächer, P. Pirro, A. A. Serga, T. Kubota, H. Naganuma, M. Oogane, Y. Ando, and B. Hillebrands, Phys. Rev. Lett. **110**, 067201 (2013).
[3]J. Hayakawaa, S. Ikeda, Y. M. Lee, F. Matsukura, and H. Ohno, Appl. Phys. Lett. **89**, 232510 (2006).
[4]S. Ikeda, J. Hayakawa, Y. Ashizawa, Y. M. Lee, K. Miura, H. Hasegawa, M. Tsunoda, F. Matsukura, and H. Ohno, Appl. Phys. Lett. **93**, 082508 (2008).
[5]C. Bilzer, T. Devolder, J.-V. Kim, G. Counil, C. Chappert, S. Cardoso, and P. P. Freitas, J. Appl. Phys. **100**, 053903 (2006).
[6]Y.-T. Chen and S. M. Xie, J. Nanomater. **2012**, 486284.
[7]S. U. Jen, T. Y. Chou, and C. Kuen Lo, Nanoscale Res. Lett. **6**, 468 (2011).
[8]C. Kittel, Phys. Rev. **73**, 155 (1948).
[9]S. S. Kalarickal, P. Krivosik, M. Wu, C. E. Patton, M. L. Schneider, P. Kabos, T. J. Silva, and J. P. Nibarger, J. Appl. Phys. **99**, 093909 (2006).
[10]M. Oogane, T. Wakitani, S. Yakata, R. Yilgin, Y. Ando, A. Sakuma, and T. Miyazaki, Jpn. J. Appl. Phys., Part 1 **45**, 3889 (2006).
[11]S. O. Demokritov and B. Hillebrands, *Spin Dynamics in Confined Magnetic Structures I* (Springer, Berlin, 2002).
[12]R. Yilgin, Y. Sakuraba, M. Oogane, S. Mizumaki, Y. Ando, and T. Miyazaki, Jpn. J. Appl. Phys., Part 2 **46**, L205 (2007).
[13]T. Kubota, S. Tsunegi, M. Oogane, S. Mizukami, T. Miyazaki, H. Naganuma, and Y. Ando, Appl. Phys. Lett. **94**, 122504 (2009).
[14]X. Liu, M. M. Steiner, R. Sooryakumar, G. A. Prinz, R. F. C. Farrow, and G. Harp, Phys. Rev. B **53**, 12166 (1996).
[15]X. Liu, R. Sooryakumar, C. J. Gutierrez, and G. A. Prinz, J. Appl. Phys. **75**, 7021 (1994).
[16]O. Gaier, J. Hamrle, S. Trudel, B. Hillebrands, H. Schneider, and G. Jakob, J. Phys. D: Appl. Phys. **42**, 232001 (2009).
[17]O. Gaier, J. Hamrle, S. Trudel, A. Conca Parra, B. Hillebrands, E. Arbelo, C. Herbort, and M. Jourdan, J. Phys. D: Appl. Phys. **42**, 084004 (2009).
[18]X. Liu, W. Zhang, M. J. Carter, and G. Xiao, J. Appl. Phys. **110**, 033910 (2011).
[19]F. Xu, Q. Huang, Z. Liao, S. Li, and K. Ong, J. Appl. Phys. **111**, 07A304 (2012).